The electron-scattering method and its applications to the structure of nuclei and nucleons

Christoph Schweiger

08. Januar 2016

Outline

I. Nuclear Structure in the 1950s

II. Elastic Electron Scattering

  i. Nuclear Structure determination

  ii. Nucleon Structure determination

III. The Proton Radius Puzzle and current research

Nuclear Structure in the 1950's

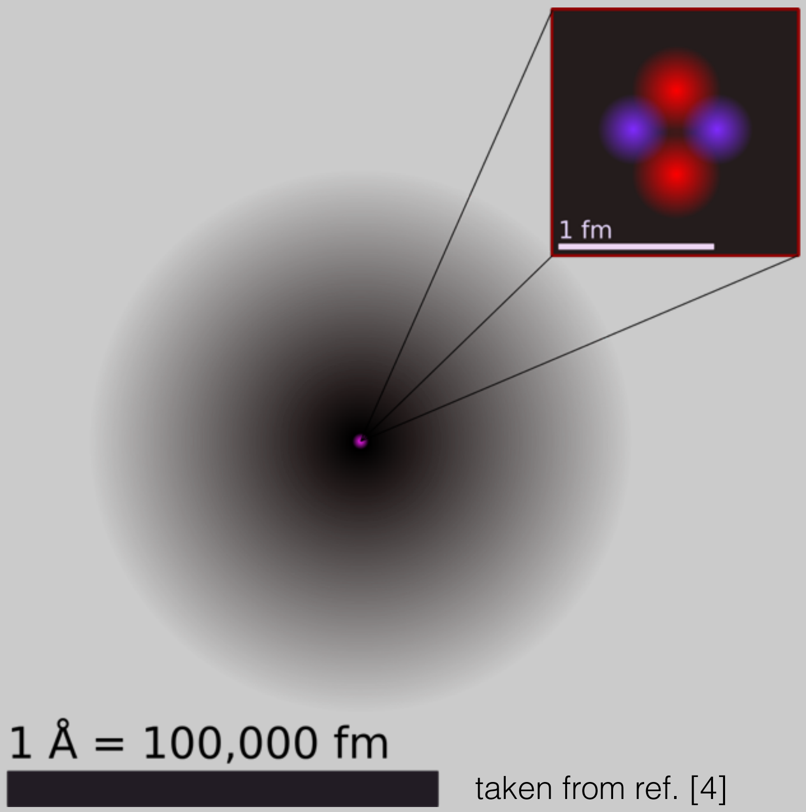

taken from ref. [4]

$$R = r_0 \cdot A^{\frac{1}{3}}\,\mathrm{fm}$$

- Rutherford: Most of the mass is located in a small, dense center of the atom => Nucleus
- Nuclei consist of protons and neutrons
- Electron scattering (up to 15.7 MeV) [3] and fast neutron scattering => Nuclei have a finite radius
- Form of the charge distribution unknown
- No knowledge of the substructure of nucleons and others than electromagnetic interaction

Robert Hofstadter

- *Feb. 5th 1915, †Nov. 17th 1990
- study of physics from 1935 at Princeton University, PhD in 1938
- from 1938 research on photoconductivity in willemite crystals and during the war at the National Bureau of Standards
- in 1950: Associate Professor at Stanford University initiating a program on electron scattering but also doing research on scintillation counters
- from 1953: Main interest in electron scattering experiments and nuclear structure
- 1961 Nobel Prize in physics

cf. ref. [1]


Ref. [1]

Structure Determination by Elastic Electron-Nucleus Scattering

- Electron is the ideal probe: point-particle and only electromagnetic interaction
- At "low" energies (< 1 GeV): elastic scattering, no disintegration of the nucleus
- Interaction type depends on de Broglie wavelength of the electron (virtual photon): elastic and inelastic scattering
- calculation of the cross-section: Born approximation and Fermi's Golden Rule

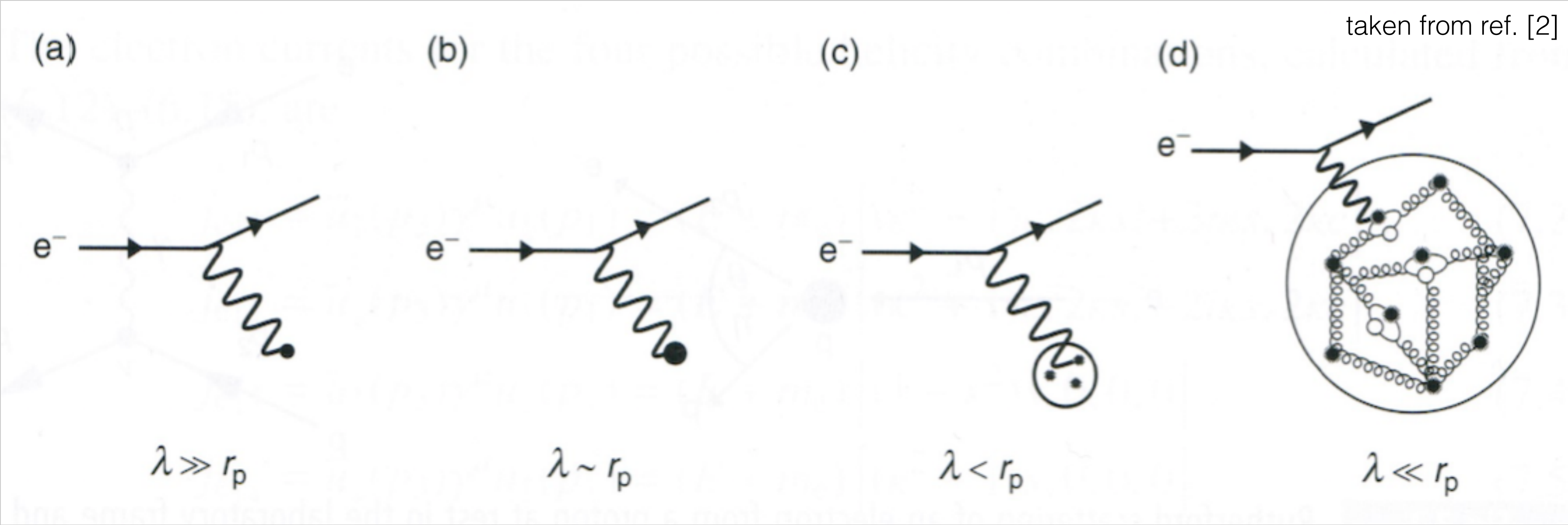

Rutherford and Mott Scattering

Rutherford scattering:

- non-relativistic, no recoil
- only interaction between electric charges
- point-like, spin-less particles

$$\left(\frac{\mathrm{d}\sigma}{\mathrm{d}\Omega}\right)_{\mathrm{R}} = \frac{\alpha^2}{16E_k^2 \sin^4\left(\frac{\theta}{2}\right)}$$

Mott scattering:

- relativistic electrons, point-like particles, recoil still negligible: $m_e \ll E \ll m_p$
- spin-less nucleus/electrons have spin
- backscattering suppressed (helicity conservation for $\beta \simeq 1$)

$$\left(\frac{\mathrm{d}\sigma}{\mathrm{d}\Omega}\right)_{\mathrm{Mott}} = \frac{\alpha^2}{16E^2 \sin^4\left(\frac{\theta}{2}\right)}\left(1 - \beta^2 \sin^2\left(\frac{\theta}{2}\right)\right)$$

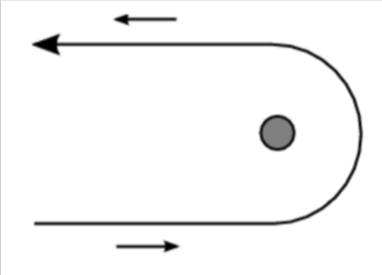

Nuclear Form Factor

- accounts for finite size of the nucleus

$$\left(\frac{\mathrm{d}\sigma}{\mathrm{d}\Omega}\right)_{\mathrm{exp}} = \left(\frac{\mathrm{d}\sigma}{\mathrm{d}\Omega}\right)_{\mathrm{Mott}} \cdot \left|F\left(\mathbf{q}^2\right)\right|^2$$

- form factor and electric charge distribution are Fourier pairs

$$F\left(\mathbf{q}^2\right) = \int \mathrm{d}^3\mathbf{r}\ \rho\left(\mathbf{r}\right) \cdot e^{i\mathbf{qr}}$$

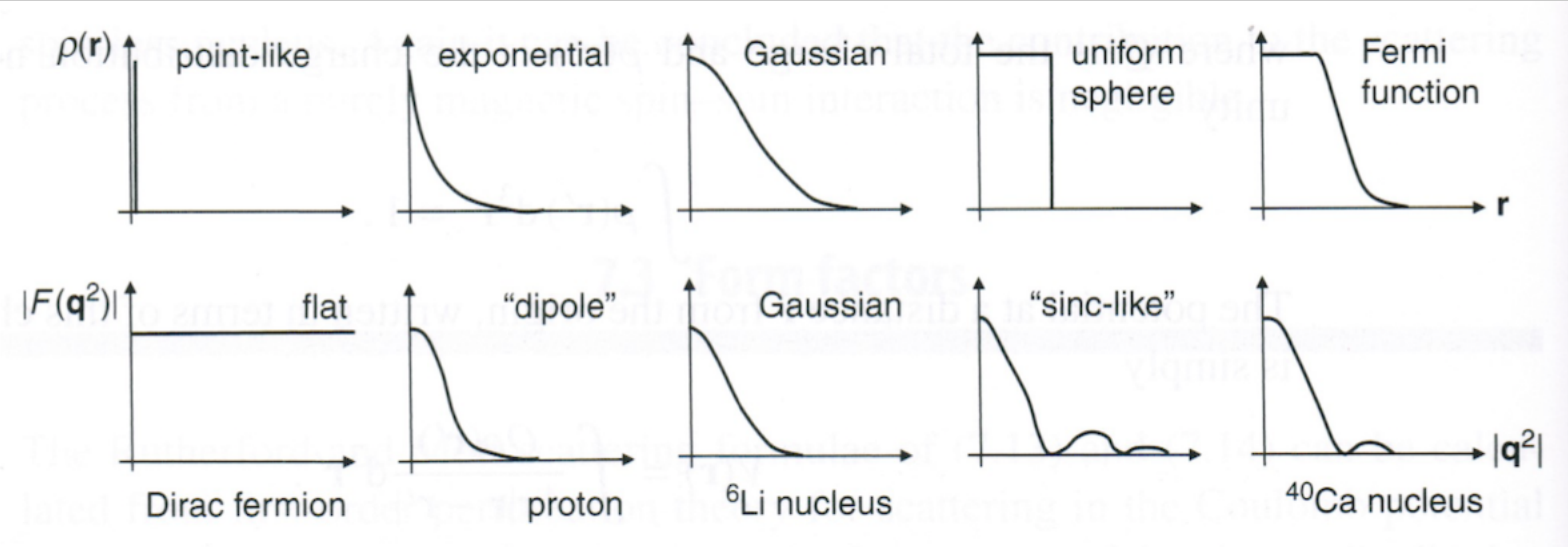

taken from ref. [2]

Experimental Apparatus

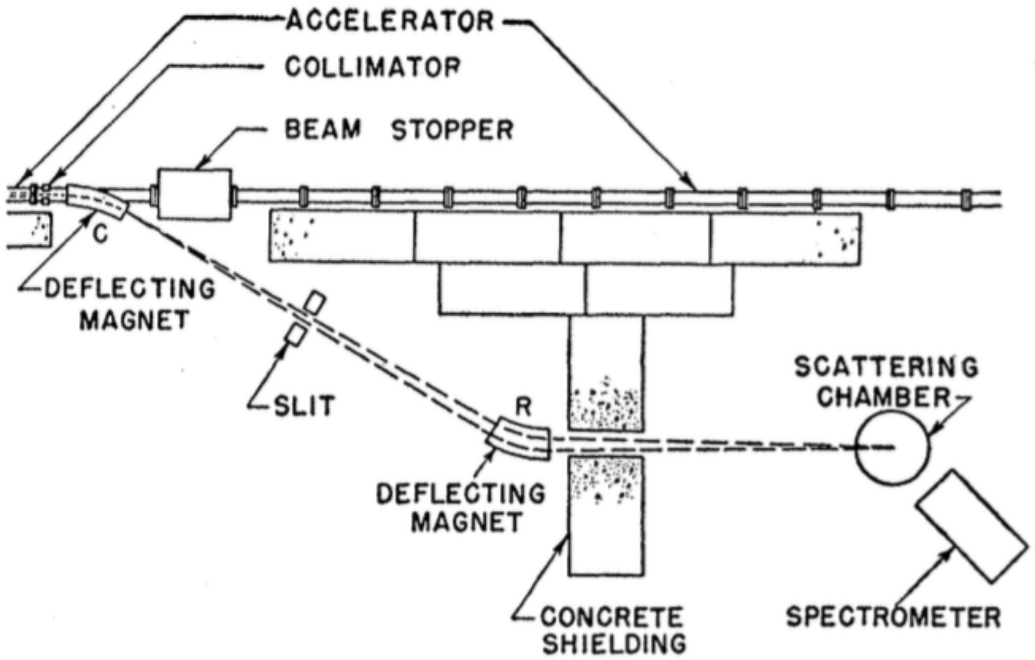

FIG. 14. The general layout of the equipment at the halfway point and the accelerator. Experiments, limited by the spectrometer to 190 Mev, are carried out in this area.

taken from ref. [7,8]

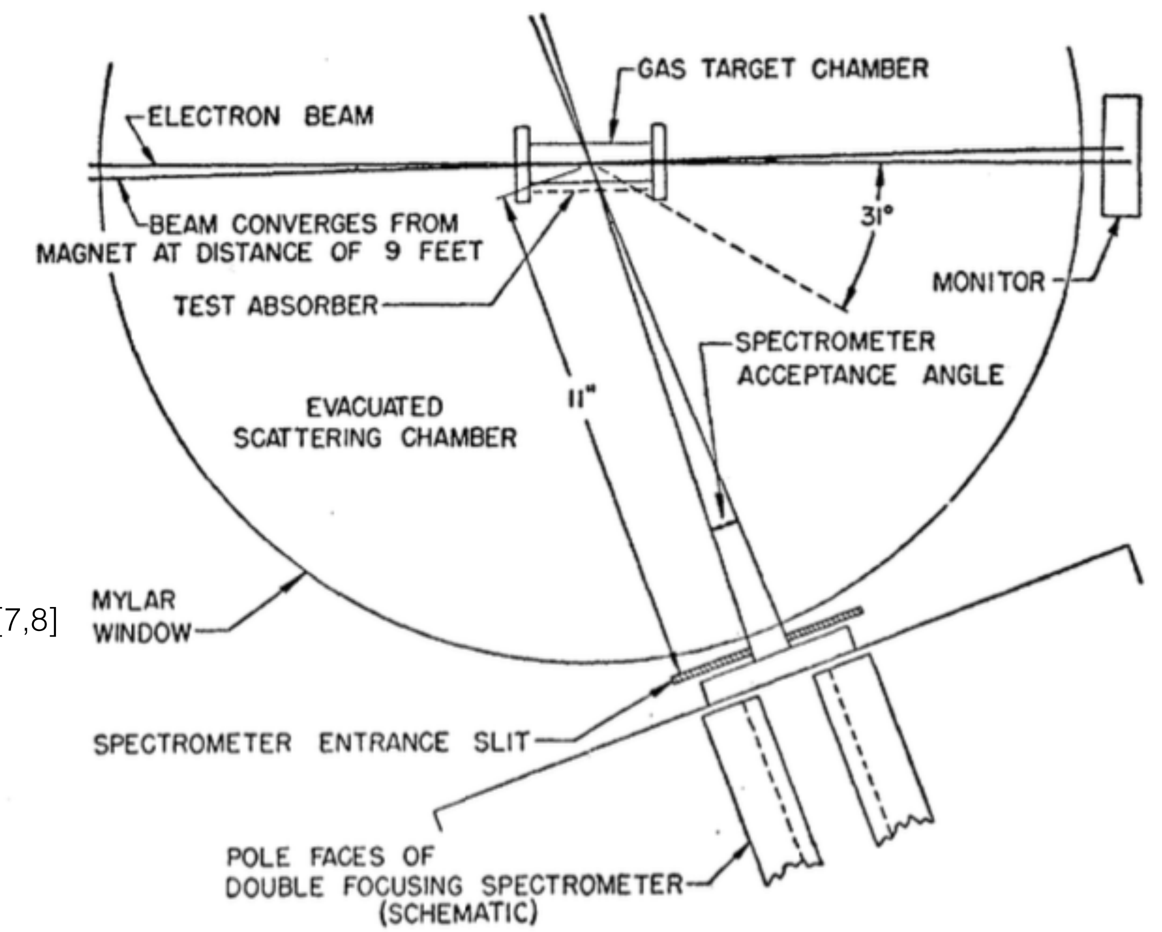

FIG. 17. Schematic diagram of scattering geometry employed with the gas target chamber.

Experimental Apparatus

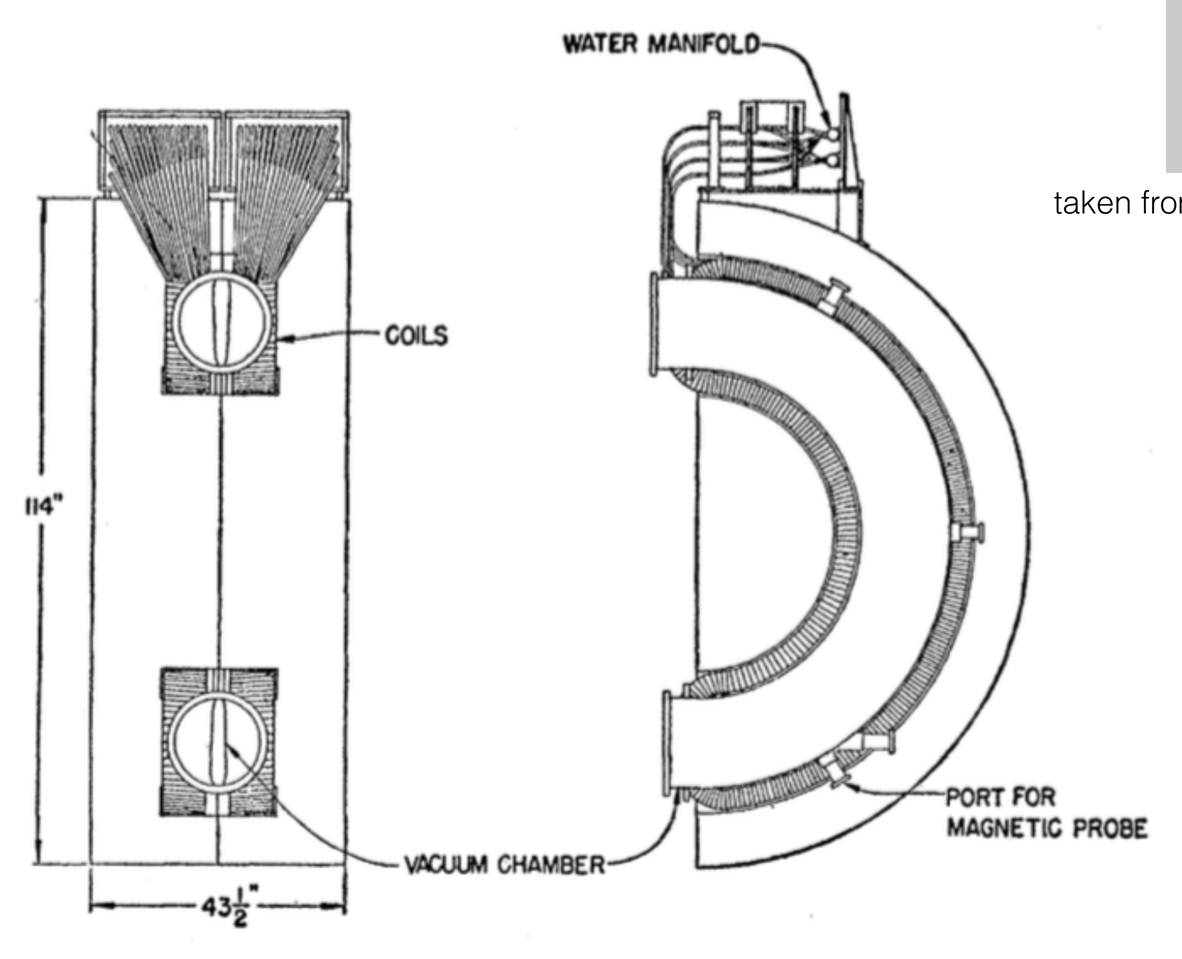

taken from ref. [7,8]

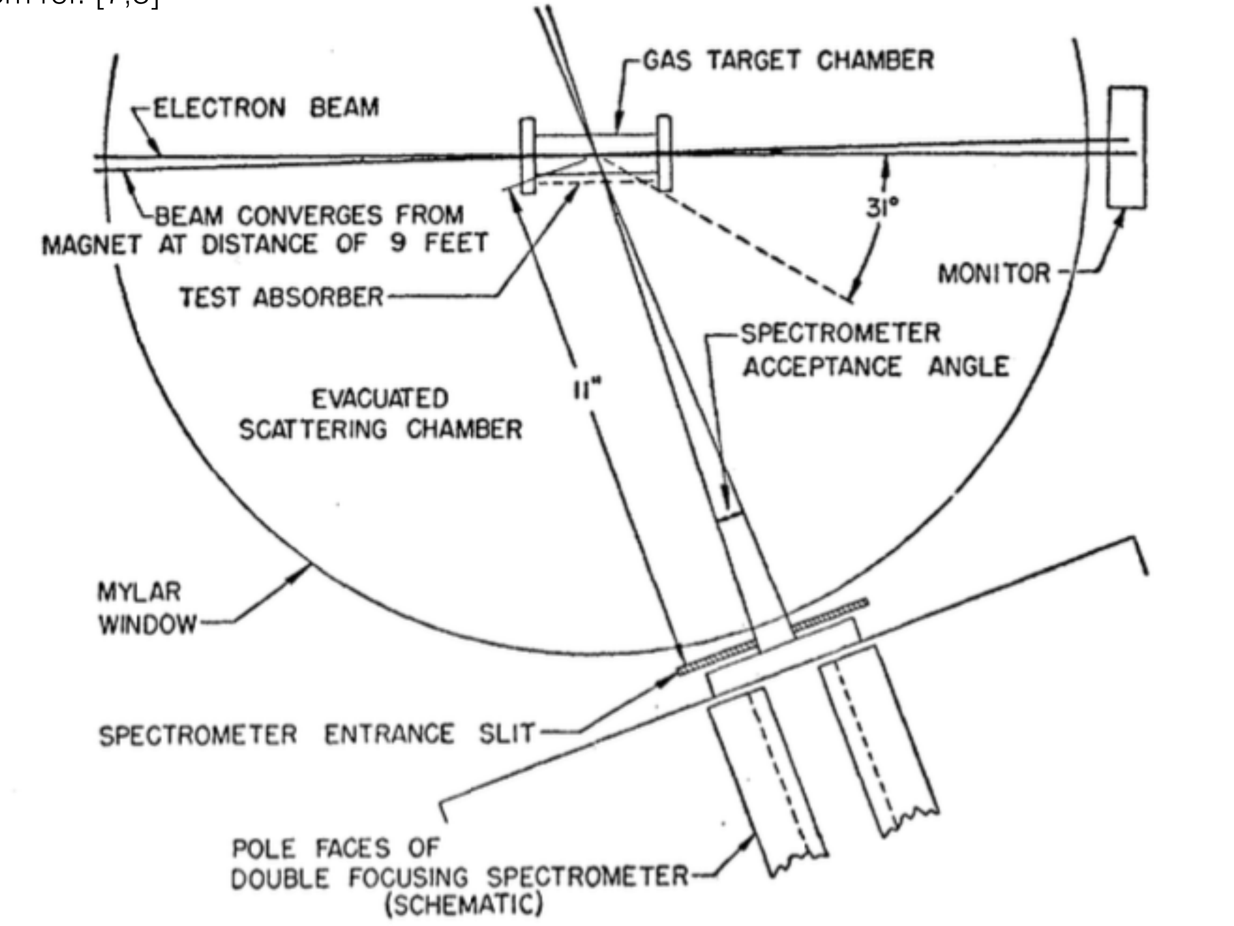

FIG. 17. Schematic diagram of scattering geometry employed with the gas target chamber.

Experimental Apparatus

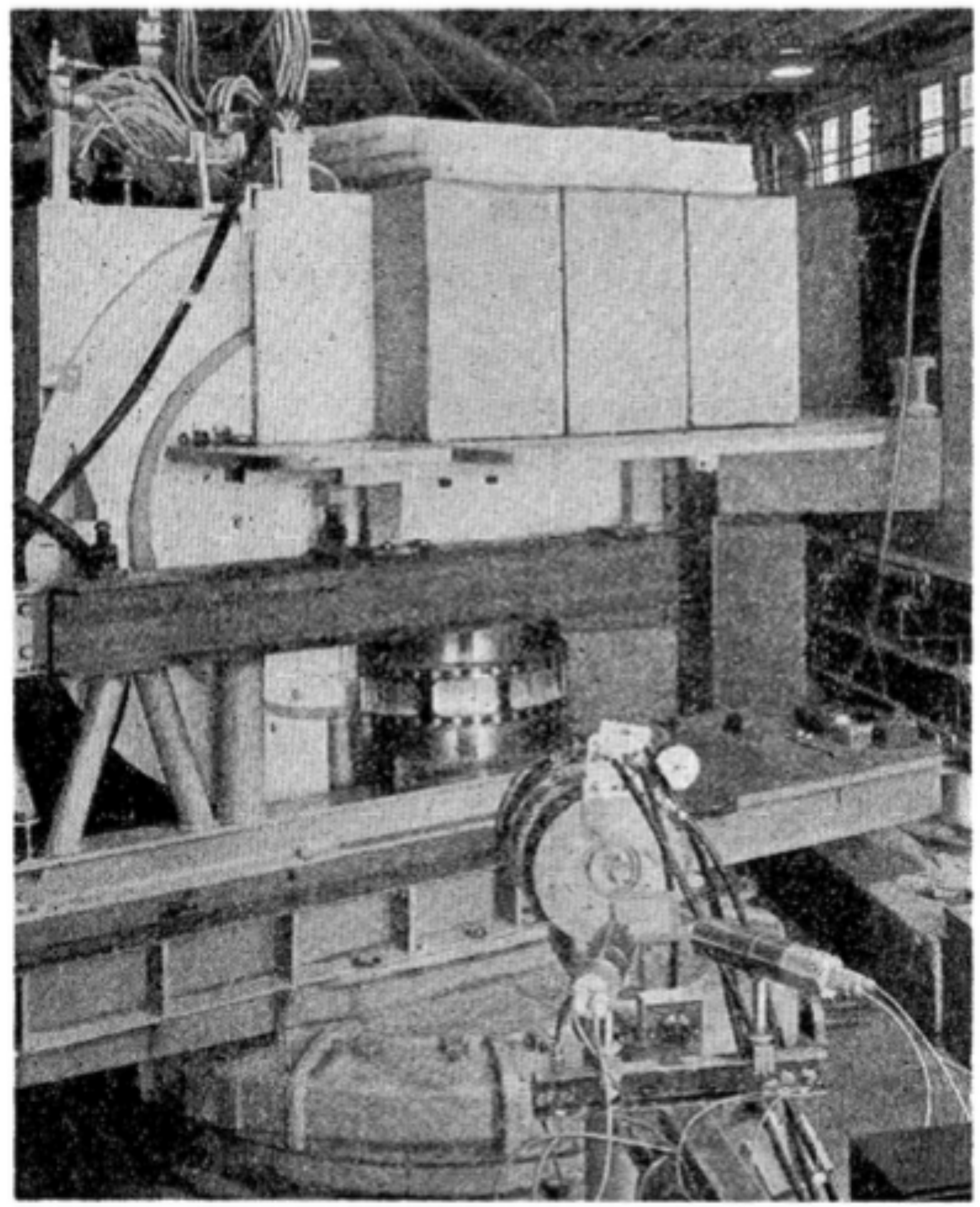

FIG. 15. The semicircular 190-Mev spectrometer, to the left, is shown on the gun mount. The upper platform carries the lead and paraffin shielding that encloses the Čerenkov counter. The brass scattring chamber is shown below with the thin window encircling it. Ion chamber monitors appear in the foreground.

taken from ref. [7]

Form Factor Measurements

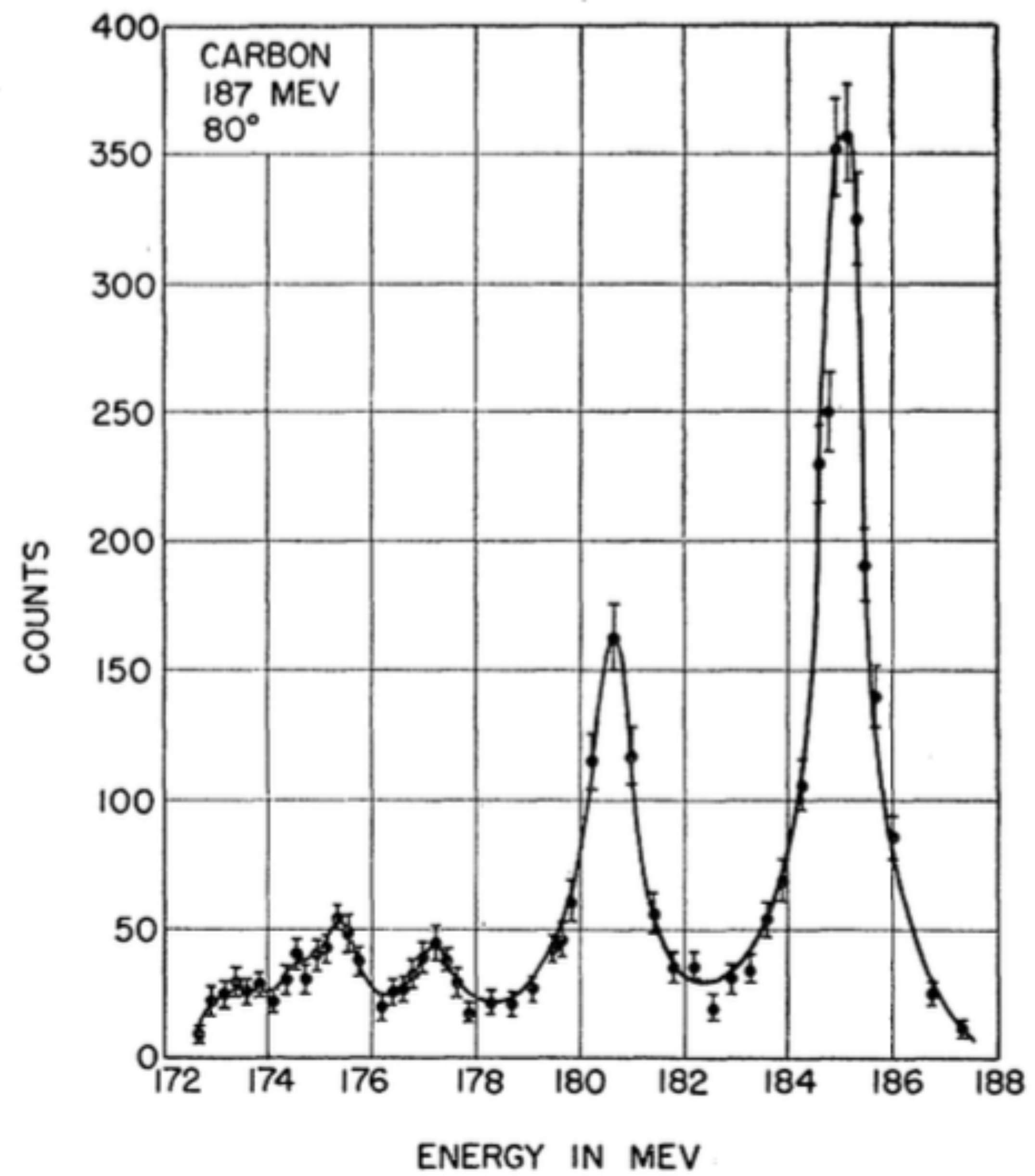

FIG. 1. The elastic and inelastic peaks at 187 Mev in carbon at a scattering angle of 80°.

taken from ref. [7,9]

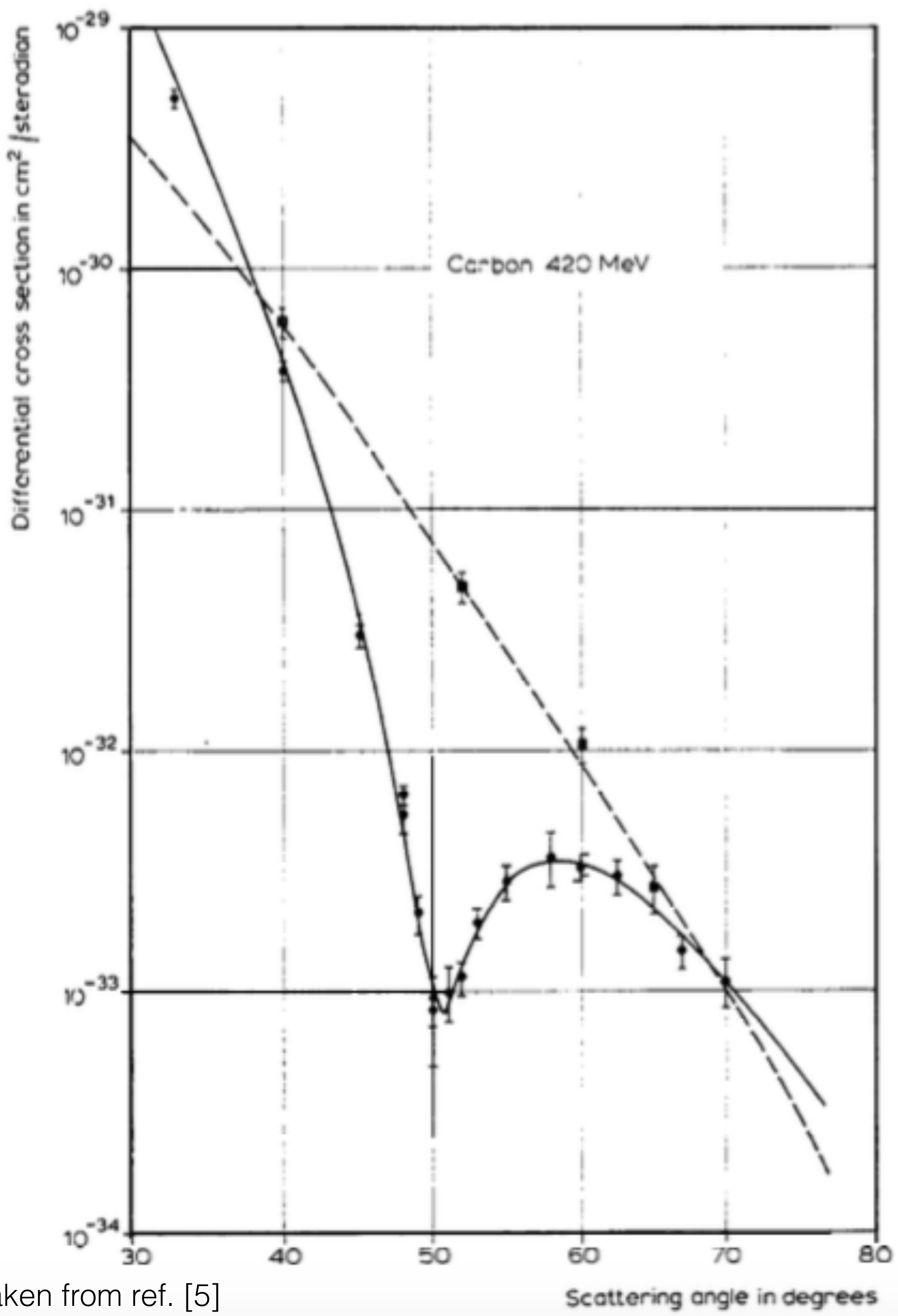

taken from ref. [5]

Form Factor Measurements

- diffraction minima of heavier elements are "washed out"

- data agree well with a Fermi-type model of the nucleus

- minima occur at the same position => $R \sim A^{\frac{1}{3}}$

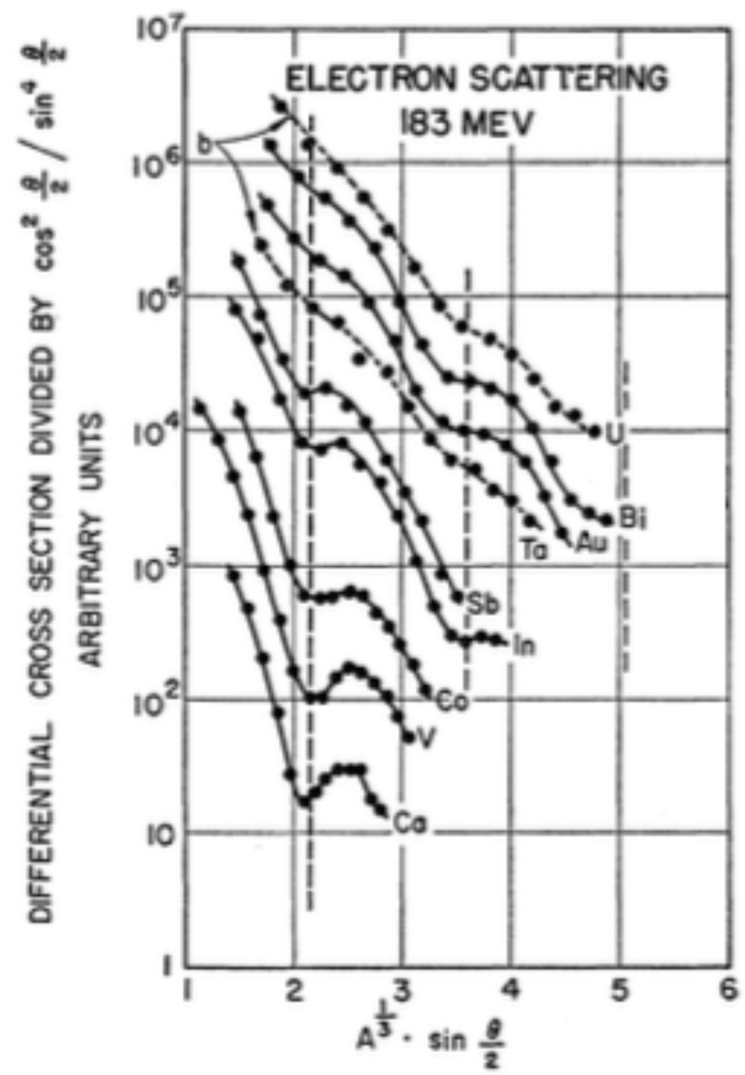

FIG. 2. Experimental results for several nuclei. The differential cross sections, divided by $\cos^2(\theta/2)/\sin^4(\theta/2)$ to display diffraction structure, are plotted *vs* $A^{\frac{1}{3}}\sin(\theta/2)$. The solid lines are smooth curves drawn through the experimental points. They have been shifted arbitrarily in the *y*-direction. The dashed vertical lines indicate approximately the location of the first, second and third diffraction dips.

taken from ref. [6]

Results on the Nuclear Charge distribution

- uniform charge distribution with smoothed surface (Fermi-model) [6,7]

- model takes only two parameters [6,7]

$$c = (1.07 \pm 0.02) \cdot A^{\frac{1}{3}} \quad \text{fm}$$
$$t = (2.4 \pm 0.3) \quad \text{fm}$$

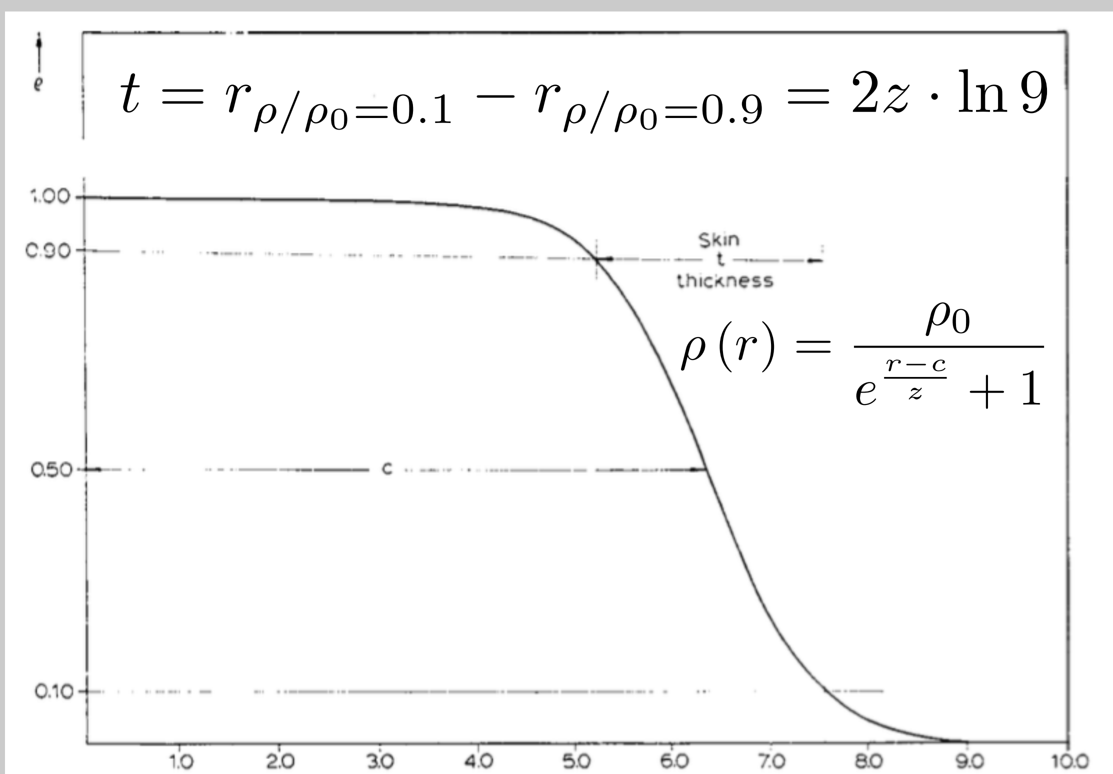

taken from ref. [5]

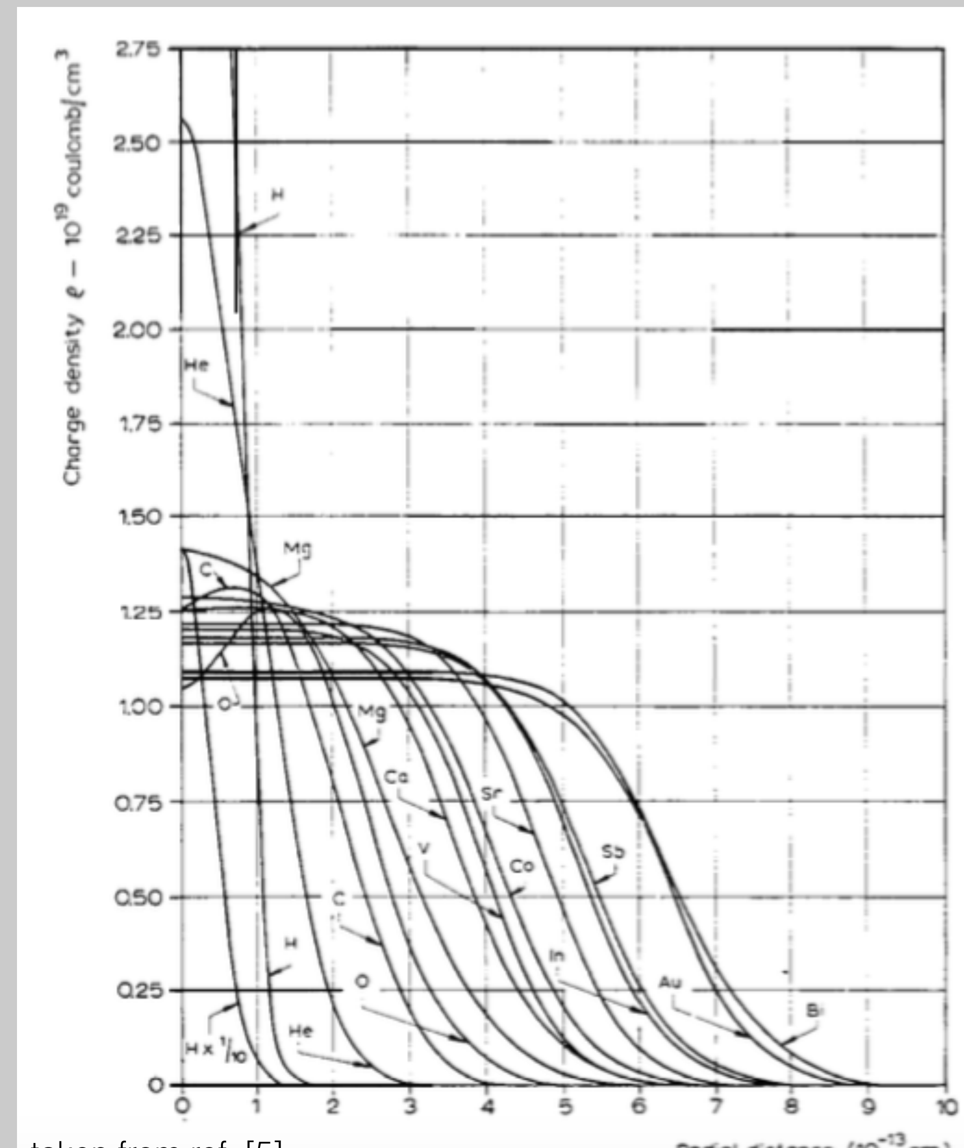

taken from ref. [5]

Results on the Nuclear Charge distribution

- uniform charge distribution with smoothed surface (Fermi-model) [6,7]
- model takes only two parameters [6,7]

$$c = (1.07 \pm 0.02) \cdot A^{\frac{1}{3}} \quad \text{fm}$$
$$t = (2.4 \pm 0.3) \quad \text{fm}$$

$$R = r_0 \cdot A^{\frac{1}{3}}\,\text{fm}$$

TABLE IV. Results of the analysis of nuclei in terms of the Fermi smoothed uniform charge distribution. All lengths are in Fermi units, charge densities in 10^{19} coulombs/cm³. The accuracy of these results is thought to be: radial parameters, ±2%; surface thickness parameter, ±10%. For lighter elements, the errors are probably larger. The accuracy for gold is higher. R is the radius of uniform charge distribution having the same rms radius as the Fermi distribution.

taken from ref. [7]

Nucleus	c	t	R	$c/A^{\frac{1}{3}}=r_1$	$R/A^{\frac{1}{3}}=r_0$
${}_{20}Ca^{40}$	3.64	2.5	4.54	1.06	1.32
${}_{23}V^{51}$	3.98	2.2	4.63	1.07	1.25
${}_{27}Co^{59}$	4.09	2.5	4.94	1.05	1.27
${}_{49}In^{115}$	5.24	2.3	5.80	1.08	1.19
${}_{51}Sb^{122}$	5.32	2.5	5.97	1.07	1.20
${}_{79}Au^{197}$	6.38	2.32	6.87	1.096	1.180
${}_{83}Bi^{209}$	6.47	2.7	7.13	1.09	1.20

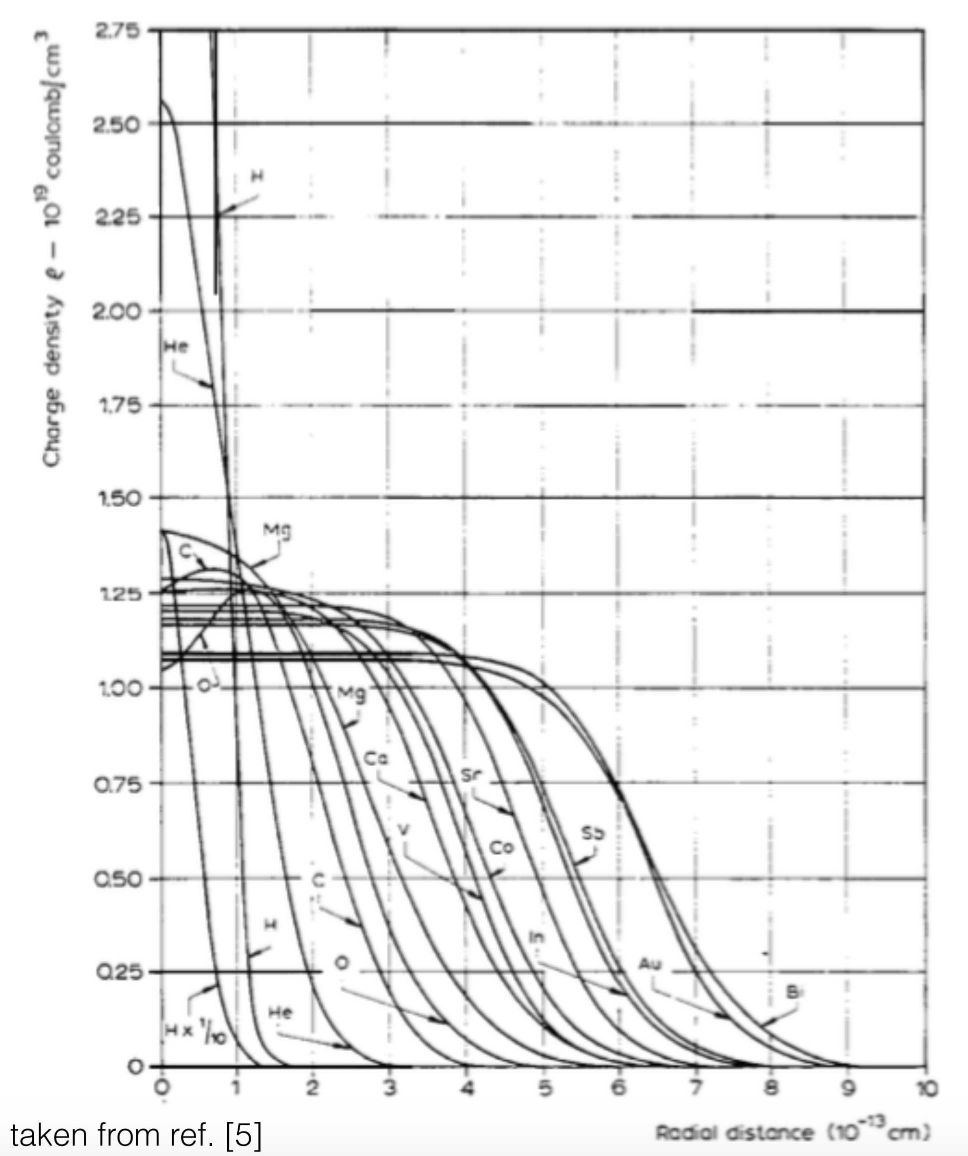

taken from ref. [5]

Nucleon Structure - How large are the Proton and Neutron?

- charge und magnetic moment distribution of proton and neutron
- idea: use electron scattering method on nucleons
- 1954: first experiments by Hofstadter showed that proton has a finite size (0.74 fm)

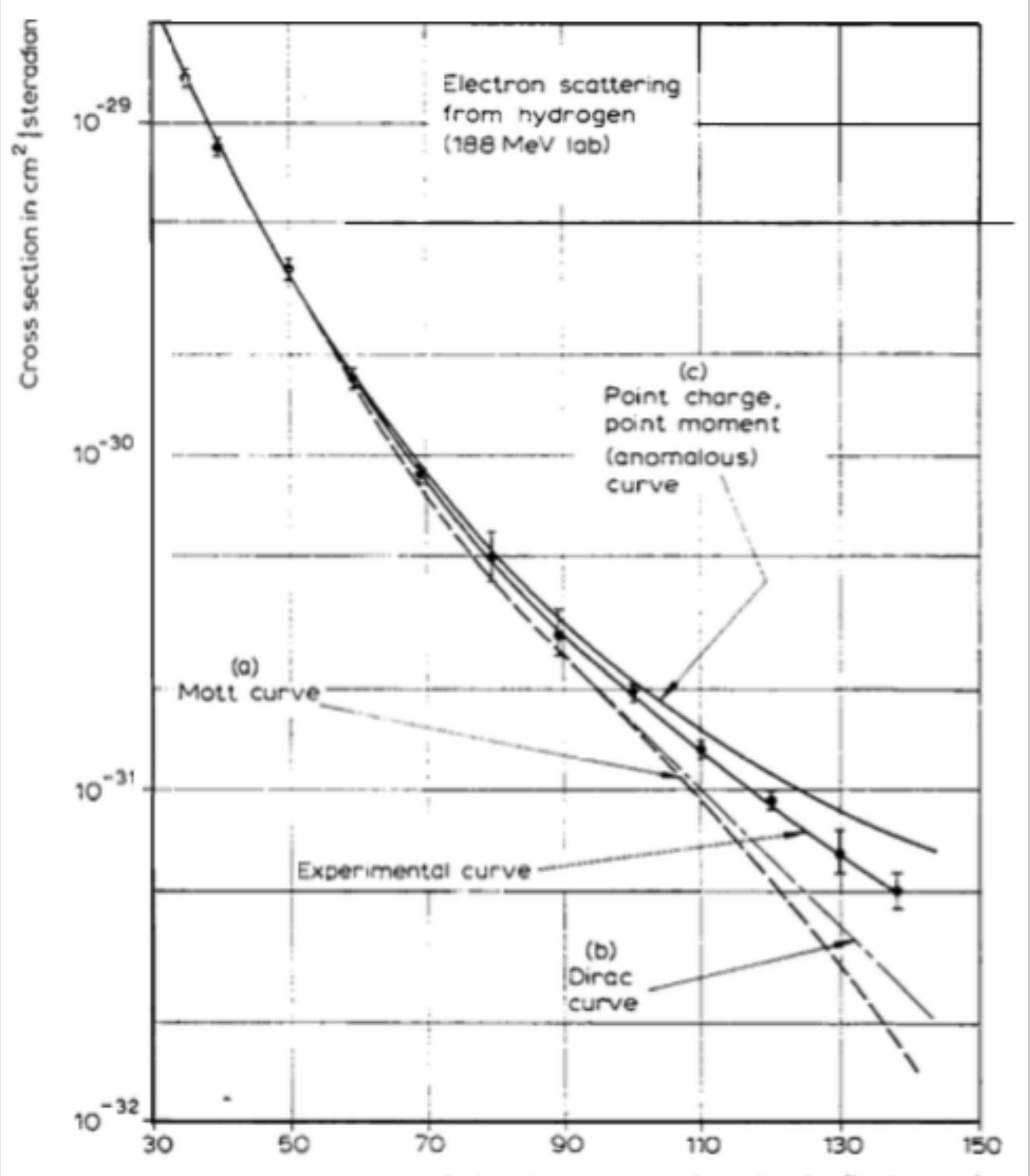

taken from ref. [5,11,12]

Rosenbluth Formula - Electric and Magnetic Form Factors cf. ref. [2]

- Rosenbluth (1950): higher electron energy -> magnetic scattering
- scattering of point-like particles with spin:

$$\left(\frac{\mathrm{d}\sigma}{\mathrm{d}\Omega}\right) = \frac{\alpha^2}{4E^2\sin^4\left(\frac{\theta}{2}\right)}\frac{E'}{E}\left(\cos^2\left(\frac{\theta}{2}\right) + \tau\sin^2\left(\frac{\theta}{2}\right)\right) \qquad \tau = \frac{Q^2}{2m_{p/n}^2}$$

- cross-section measurement: counting number of electrons scattered in a particular direction and knowing the incident electron flux
- account for finite size of the nucleons (Rosenbluth formula):

$$\left(\frac{\mathrm{d}\sigma}{\mathrm{d}\Omega}\right)_{\mathrm{Rosenbluth}} = \left(\frac{\mathrm{d}\sigma}{\mathrm{d}\Omega}\right)_{\mathrm{R}}\frac{E'}{E}\cdot\left(\frac{G_E^2+\tau G_M^2}{1+\tau}\cos^2\left(\frac{\theta}{2}\right) + 2\tau G_M^2\sin^2\left(\frac{\theta}{2}\right)\right)$$

Electric and Magnetic Form Factor

cf. ref. [2]

- Fourier-transforms of the charge/magnetic moment distribution in the limit $Q^2 \ll 4m_p^2 \quad \Rightarrow \quad Q^2 \simeq \mathbf{q}^2$

$$G_E(Q^2) \simeq G_E(\mathbf{q}^2) = \int \mathrm{d}^3\mathbf{r}\, \rho(\mathbf{r})\, e^{i\mathbf{qr}}$$

$$G_M(Q^2) \simeq G_M(\mathbf{q}^2) = \int \mathrm{d}^3\mathbf{r}\, \mu(\mathbf{r})\, e^{i\mathbf{qr}}$$

- normalisation of the form factors to the charge/magnetic moment:

$$G_E^p(Q^2 = 0) = 1 \qquad G_E^n(Q^2 = 0) = 0$$

$$G_M^p(Q^2 = 0) = 2.79 \qquad G_M^n(Q^2 = 0) = -1.91$$

Dirac- and Pauli Form Factors

- relation to electric and magnetic form factors

$$G_E = F_1 - \tau F_2 \qquad\qquad G_M = F_1 + F_2$$

- F_1 Dirac form factor: spread out charge distribution and magnetic moment

- F_2 Pauli form factor: anomalous magnetic moment ($\mu = 1.79$)

$$\sigma = \frac{e^4}{4E^2}\left(\frac{\cos^2\left(\frac{\theta}{2}\right)}{\sin^4\left(\frac{\theta}{2}\right)}\right)\frac{1}{1+\frac{2E}{m_p}\sin^2\left(\frac{\theta}{2}\right)}\cdot\left\{F_1^2 + \frac{q^2}{4m_p^2}\left[2\left(F_1+\mu F_2\right)^2\right]\tan^2\left(\frac{\theta}{2}\right) + \mu^2 F_2^2\right\}$$

$$\begin{aligned} F_1^p &= 1 & F_1^n &= 0 \\ F_2^p &= 1.79 & F_2^n &= -1.91 \end{aligned}$$

Proton Structure Results I (1956) [13,14]

$$\rho(r) = \rho_0 e^{-\frac{r}{R_{rms}}}$$

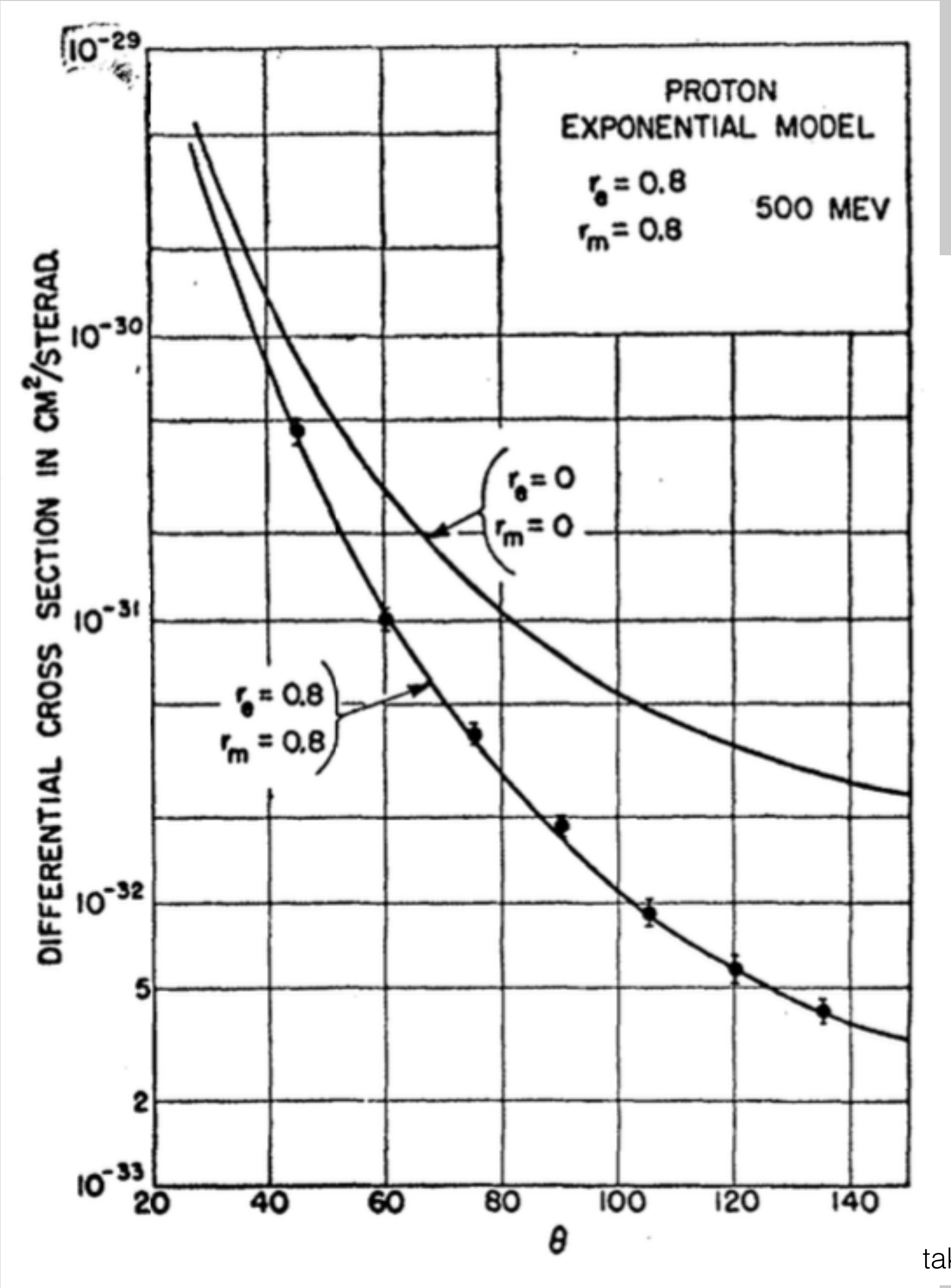

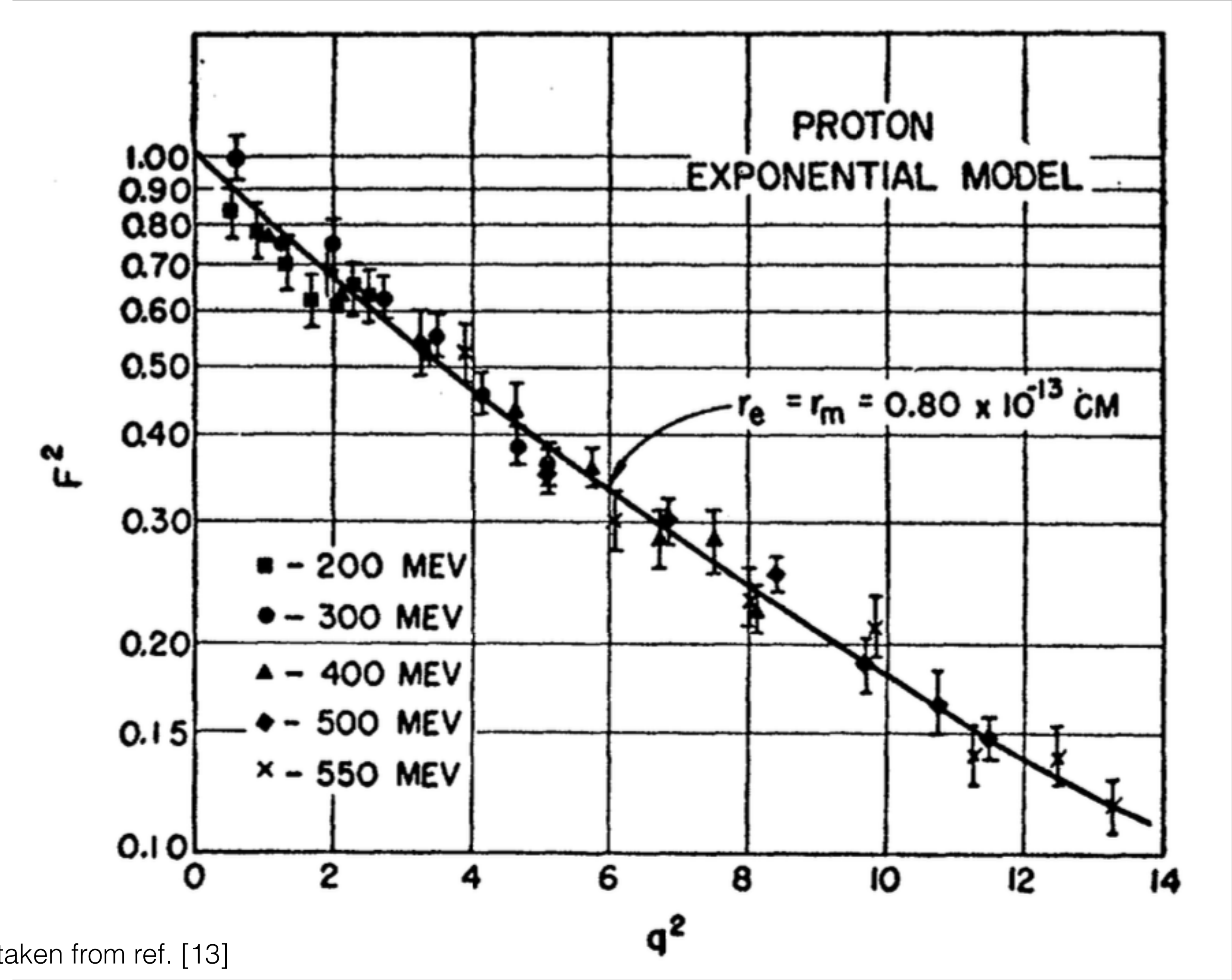

taken from ref. [13]

Proton Structure Results II (1961)

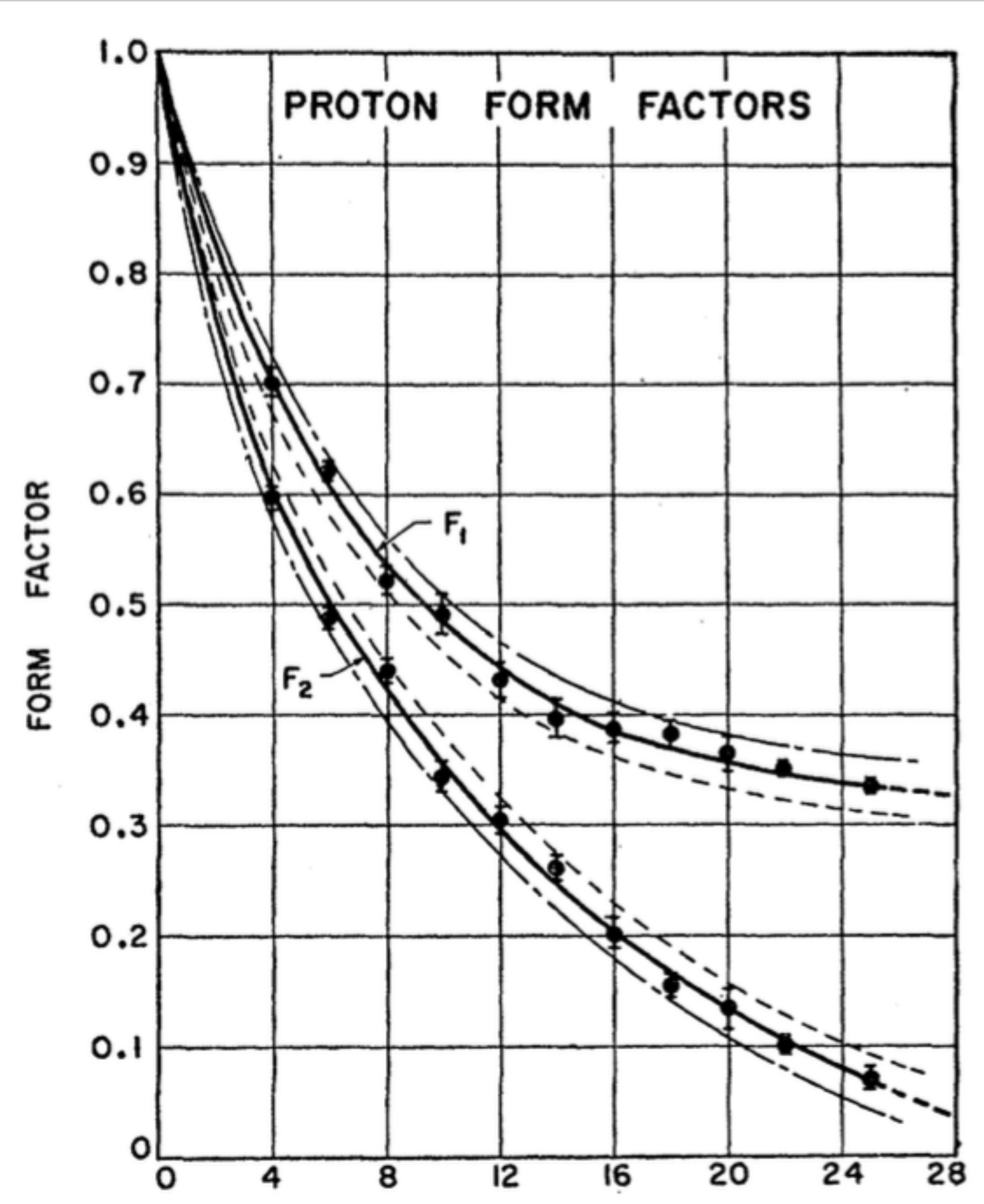

taken from ref. [15]

- form factors split at higher momentum transfer
- charge and magnetic moment RMS radii can be extracted independent of the distribution model

$$\langle r^2 \rangle = \left[-6 \frac{\mathrm{d}F_1(\mathbf{q}^2)}{\mathrm{d}\mathbf{q}^2} \right]_{\mathbf{q}^2=0}$$

- results as of 1961 [cf. ref. 15]:

$$R_c = (0.75 \pm 0.05)\,\mathrm{fm}$$
$$R_m = (0.97 \pm 0.10)\,\mathrm{fm}$$

The Structure of the Neutron

- neutrons only available in the deuteron
- at large momentum transfer neutron essentially free
- cross section approx. sum of proton and neutron cross section

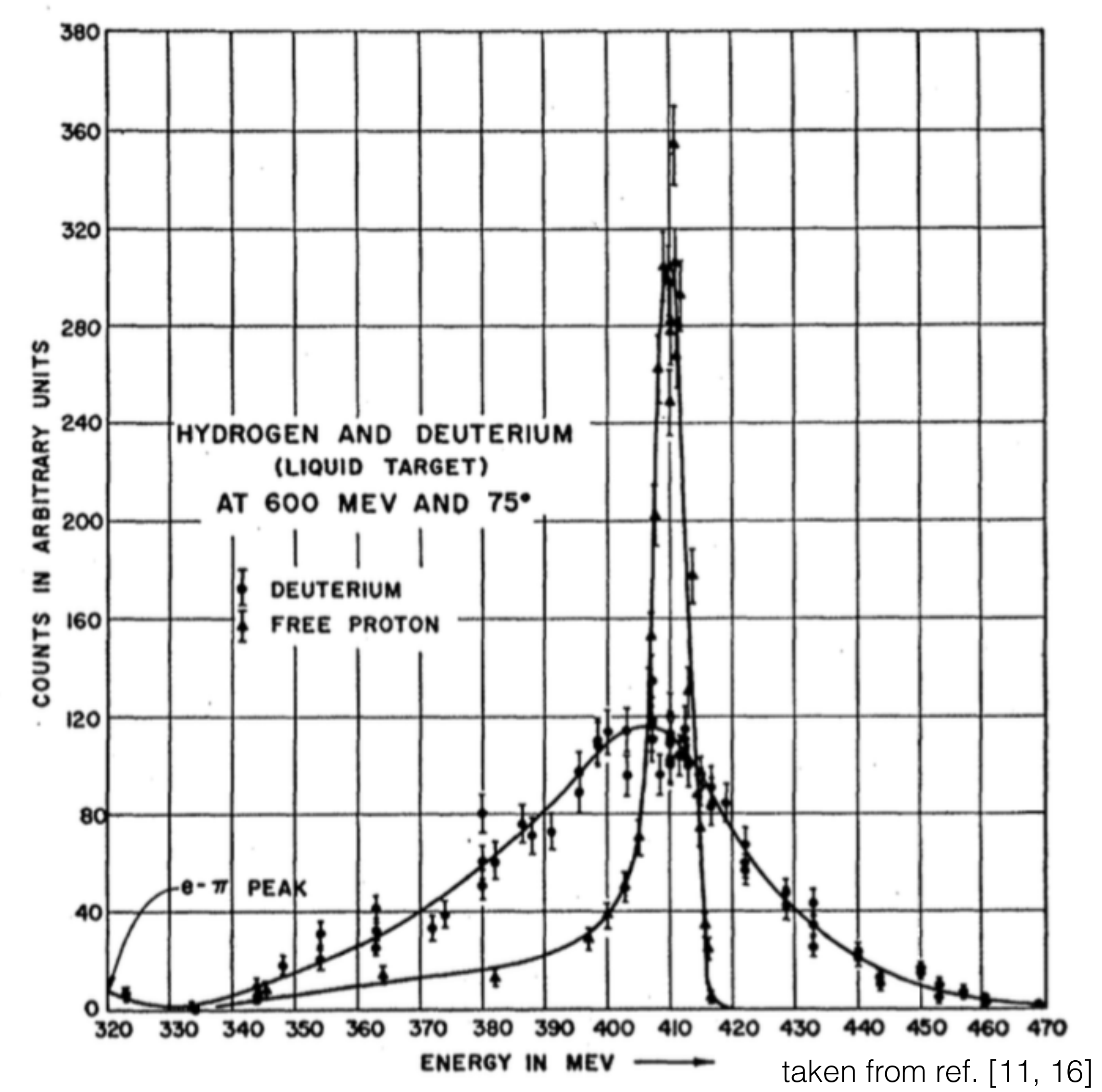

taken from ref. [11, 16]

The Structure of the Neutron

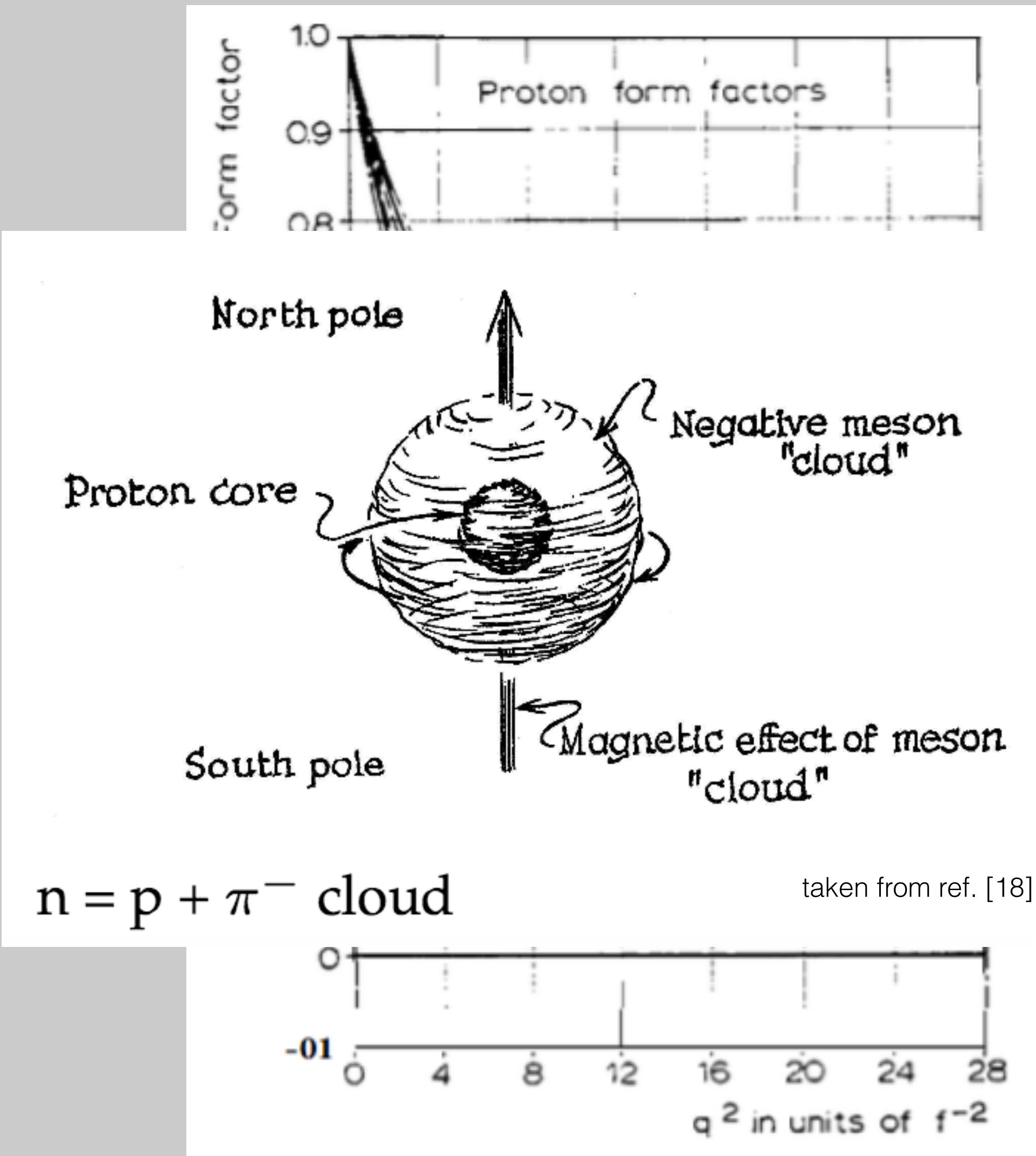

$\mathrm{n} = \mathrm{p} + \pi^{-}$ cloud

taken from ref. [18]

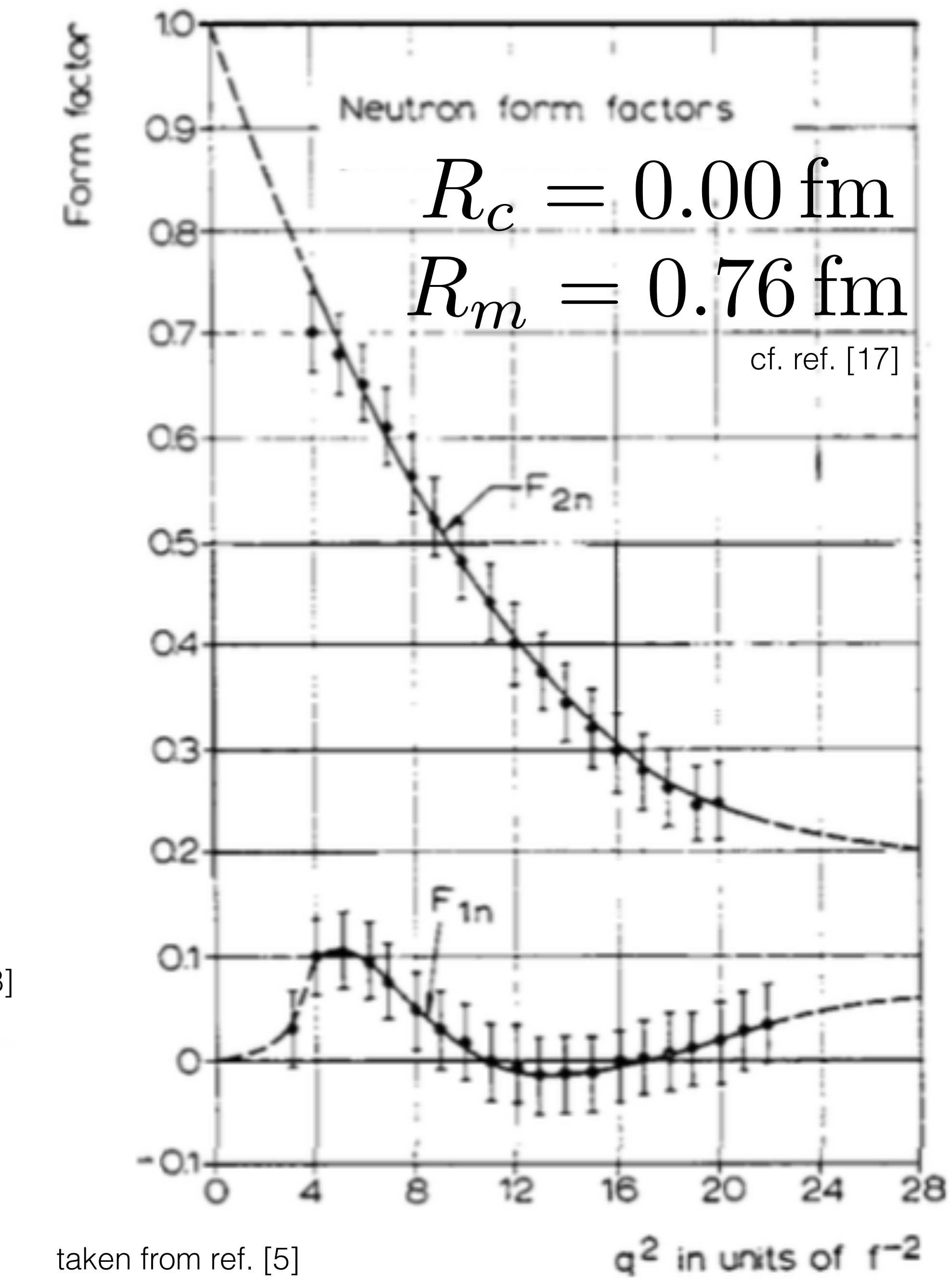

$$R_c = 0.00\,\mathrm{fm}$$
$$R_m = 0.76\,\mathrm{fm}$$

cf. ref. [17]

taken from ref. [5]

The Proton Radius - Today

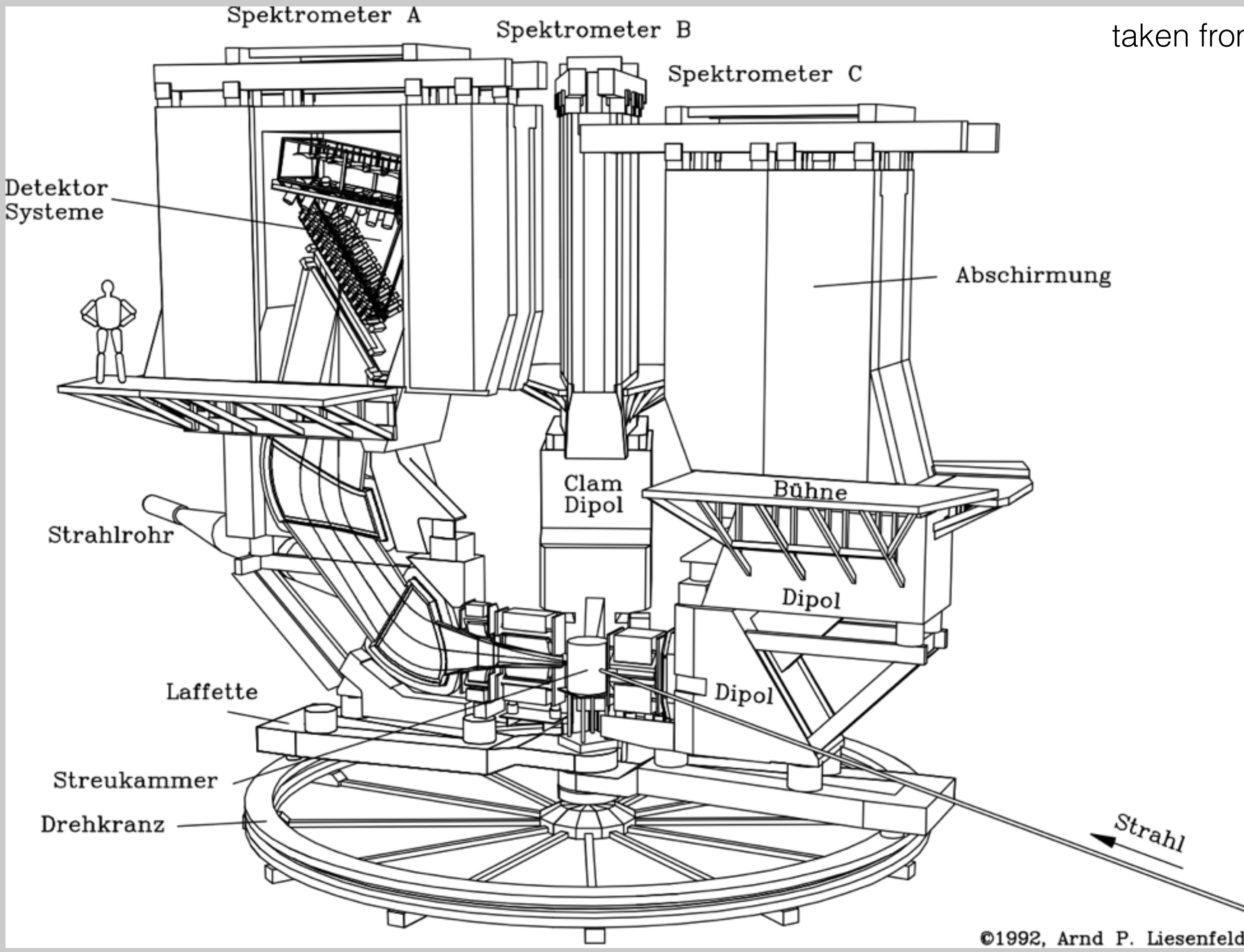

taken from ref. [19]

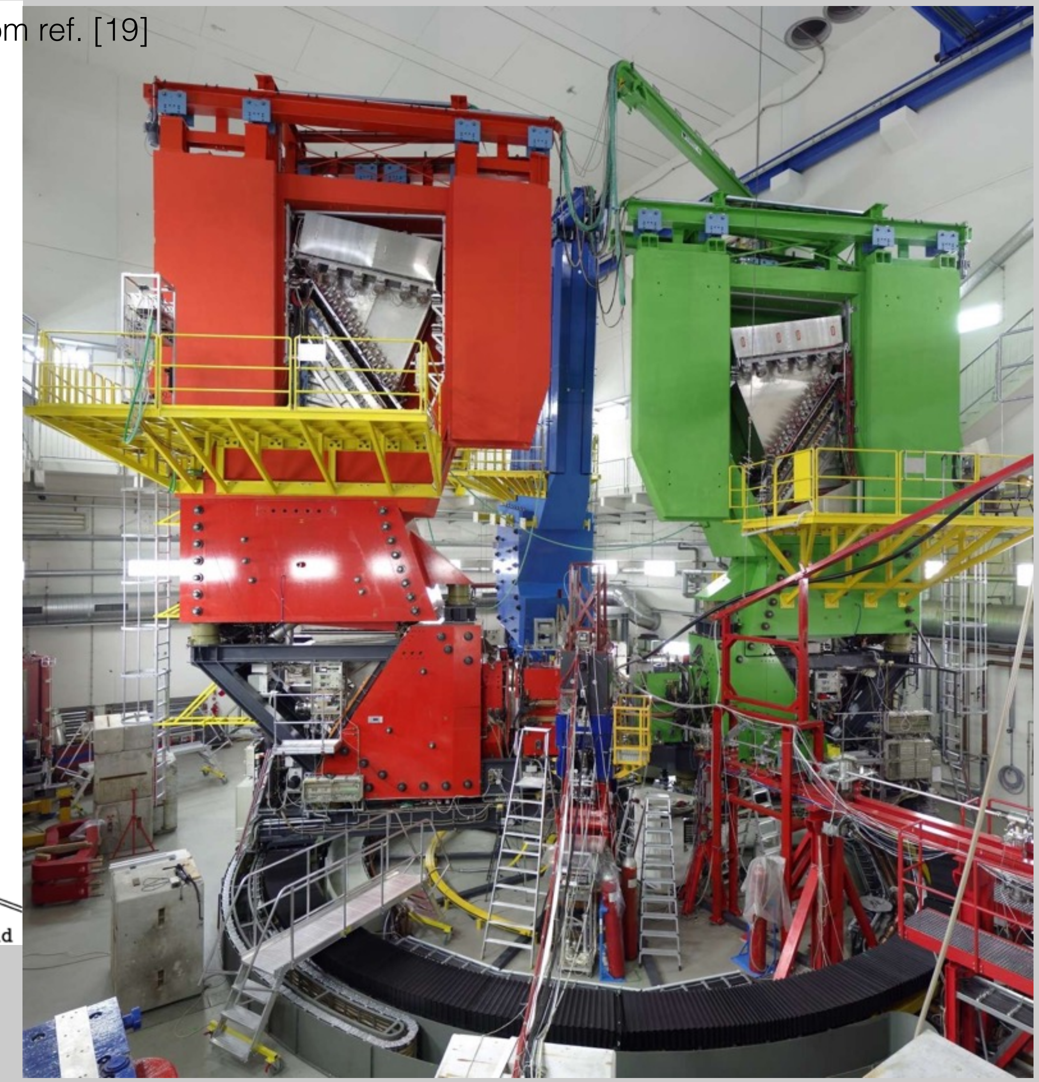

$$R_c = 0.879(5)_{\text{stat.}}(5)_{\text{syst.}}(2)_{\text{model}}(4)_{\text{group}}\ \text{fm}$$

$$R_m = 0.777(13)_{\text{stat.}}(9)_{\text{syst.}}(5)_{\text{model}}(2)_{\text{group}}\ \text{fm}$$

cf. ref. [20]

The Proton Radius Puzzle

The proton radius measured by spectroscopy of muonic hydrogen differs by 7σ from the proton radius obtained using the electron scattering method and spectroscopy of "normal" hydrogen.

The atomic orbit of the muon is much closer to the proton since $\frac{m_\mu}{m_e} \simeq 200$

=> higher sensitivity of the muon energy levels to the proton size [21,22]

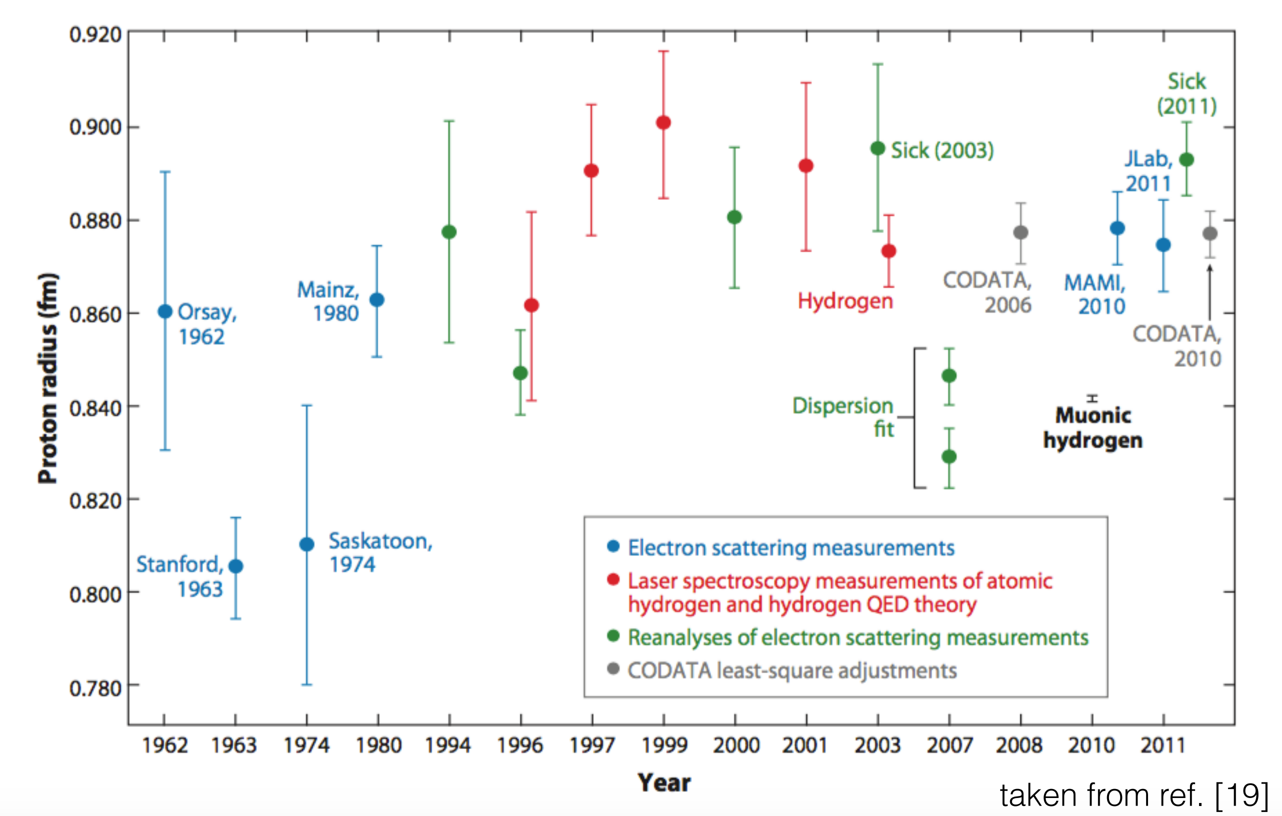

taken from ref. [19]

$$R_c = 0.84087(39)\ \mathrm{fm}$$
$$R_m = 0.87(6)\ \mathrm{fm}$$

cf. ref. [22]

$$R_c^{ref} = 0.8791(79)\ \mathrm{fm}$$
$$R_m^{ref} = 0.803(17)\ \mathrm{fm}$$

cf. ref. [23,24,26]

Summary - Electron Scattering

- nuclei have Fermi-type charge distribution described by two parameters, the radius c which depends on the number of nucleons and a surface thickness t which is constant for all nuclei
- nucleons have a finite size and can be described by an exponential charge/magnetic moment distribution
- development of the electron scattering method which is used today to measure the form factors of nuclei/ nucleons

Questions?

Thank you for your attention!

Measurement of the Form Factors

$$\left(\frac{\mathrm{d}\sigma}{\mathrm{d}\Omega}\right) = \left(\frac{\mathrm{d}\sigma}{\mathrm{d}\Omega}\right)_{\mathrm{Mott}} \cdot \left[\frac{G_{\mathrm{E}}^2(Q^2) + \tau G_{\mathrm{M}}^2(Q^2)}{1+\tau} + 2\tau G_{\mathrm{M}}^2(Q^2)\tan^2\frac{\theta}{2}\right]$$

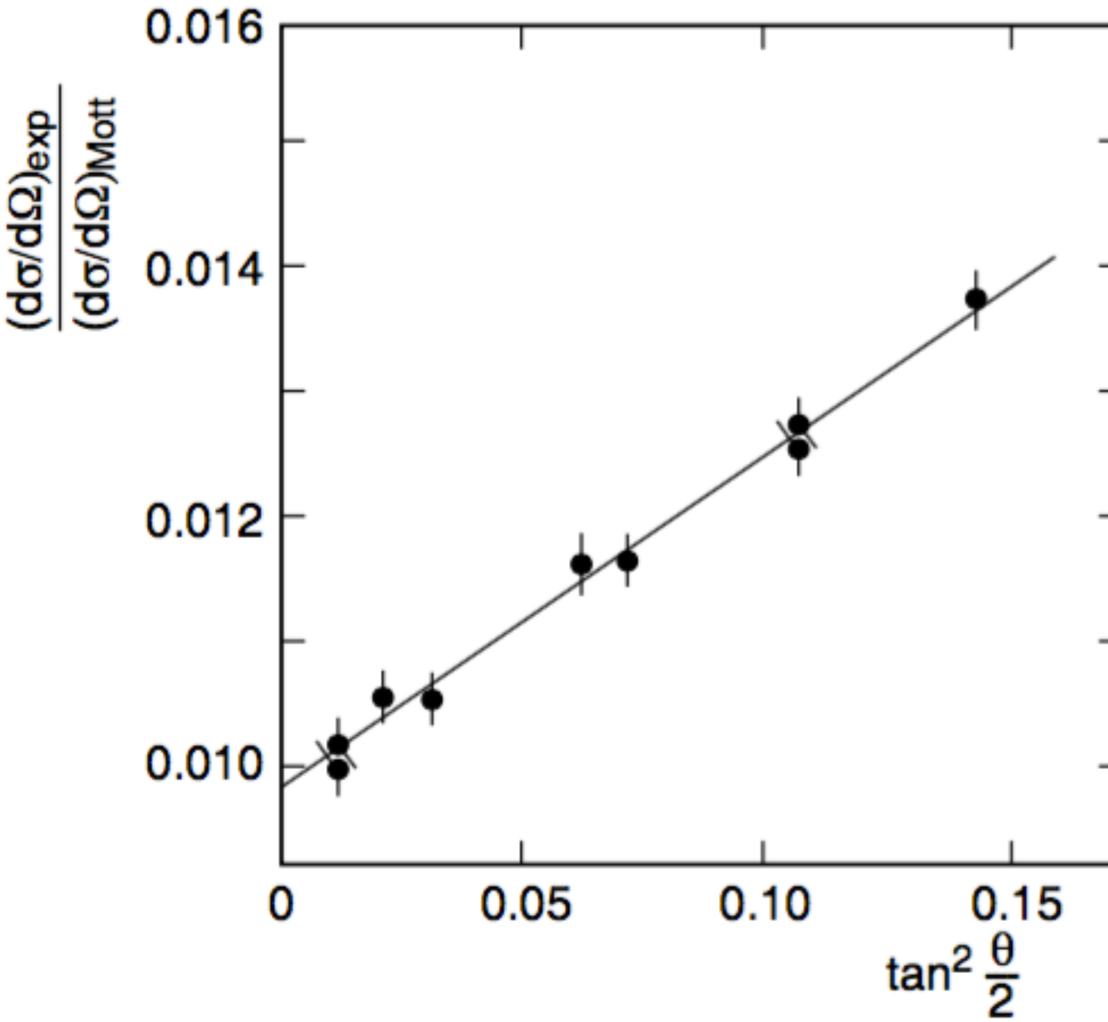

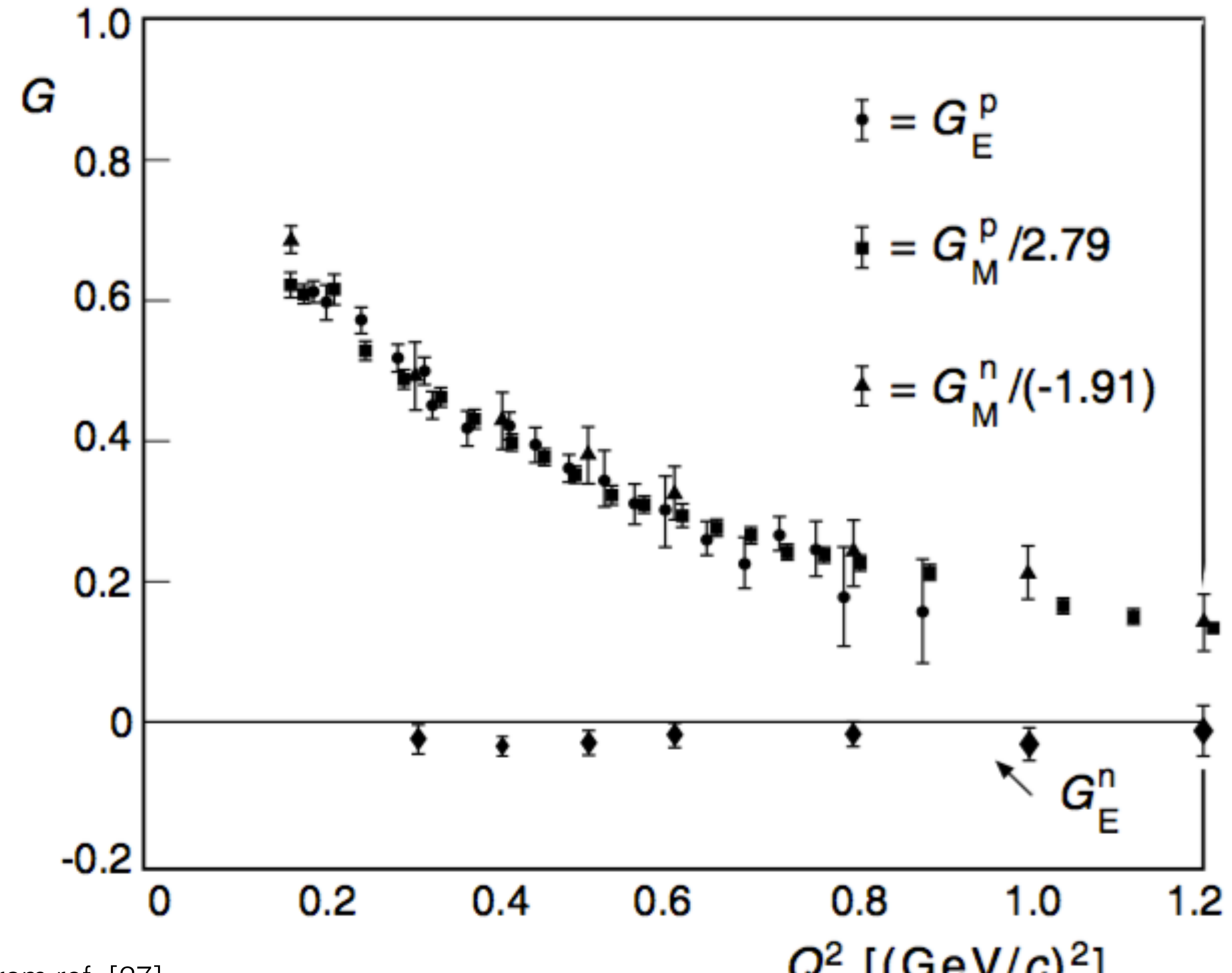

taken from ref. [27]

References I

[1] http://www.nobelprize.org/nobel_prizes/physics/laureates/1961/hofstadter-bio.html (12/30/2015)

[2] Thomson, M.: Modern Particle Physics, Cambridge University Press, 2013

[3] Lyman et al., Phys. Rev. 84, 626 (1951)

[4] https://en.wikipedia.org/wiki/Atomic_nucleus#Nuclear_models (12/29/2015)

[5] Hofstadter, R.: The electron-scattering method and its application to the structure of nuclei and nucleons, Nobel Lecture, 1961, http://www.nobelprize.org/nobel_prizes/physics/laureates/1961/hofstadter-lecture.html (12/30/2015)

[6] Hahn, B. et al., Phys. Rev. 101, 1131 (1955)

[7] Hofstadter, R., Rev. Mod. Phys. 28, 214 (1956)

[8] Hofstadter, R. et al., Phys. Rev..92, 978 (1953)

[9] Fregeau, J.H. et al., Phys. Rev. 99, 1503 (1955)

[10] Hofstadter, R. et al., Phys. Rev. 98, 217 (1955)

References II

[11] Hofstadter, R. et al., Rev. Mod. Phys. 30, 482 (1958)

[12] Hofstadter, R. et al., Phys. Rev. 98, 217 (1955)

[13] Chambers, E.E. et al., Phys. Rev. 103, 1454 (1956)

[14] McAllister,, R.W. et al., Phys. Rev. 102 851 (1956)

[15] Bumiller, F. et al., Phys. Rev. 124, 1623 (1961)

[16] Yearian, M.R. et al., Phys. Rev. 110, 552 (1958)

[17] Hofstadter, R. et al., Phys. Rev. Lett. 6, 293 (1961)

[18] http://people.virginia.edu/~dbd/NPTalks/Greensboro.pdf (01/03/2016)

[19] http://wwwa1.kph.uni-mainz.de/A1/gallery/ (01/03/2016)

[20] Bernauer, J.C. et al., Phys. Rev. C 90, 015206 (2014) and Bernaber, J.C. et al. Phys. Rev. Lett. 105, 242001 (2010)

References III

[21] https://www.psi.ch/media/proton-size-puzzle-reinforced (01/03/2016)

[22] Antognini, A. et al., Science 339, 417 (2013) and Pohl, R. et al. Nature Letters 466, 213 (2010)

[23] Mohr, P.J. et al., Rev. Mod. Phys. 84, 1527 (2012)

[24] Zhan, X. et al., Phys. Lett. B 705, 59 (2011)

[25] Pohl, R. et al., Annu. Rev. Nucl. Part. Sci. 63, 175 (2013)

[26] Bernauer, J.C. et al., Phys. Rev. Lett. 107, 119102 (2011)

[27] Povh, B. et al.: Teilchen und Kerne, Springer Lehrbuch, 8. Auflage, 2009